Inferences from Simple Models of Slow, Convectively Coupled Processes

Citation: Emanuel, Kerry Andrew, "Inferences from Simple Models of Slow, Convectively Coupled Processes." Journal of the Atmospheric Sciences 76, 1 (January 2019): p.195-208 DOI 10.1175/JAS-D-18-0090.1 ©2019 Author(s)

As Published: 10.1175/JAS-D-18-0090.1

Publisher: American Meteorological Society

Persistent URL: https://hdl.handle.net/1721.1/125071

Version: Final published version: final published article, as it appeared in a journal, conference proceedings, or other formally published context

Inferences from Simple Models of Slow, Convectively Coupled Processes

KERRY EMANUEL

Lorenz Center, Massachusetts Institute of Technology, Cambridge, Massachusetts

(Manuscript received 20 March 2018, in final form 28 October 2018)

ABSTRACT

A framework for conceptual understanding of slow, convectively coupled disturbances is developed and applied to several canonical tropical problems, including the water vapor content of an atmosphere in radiative–convective equilibrium, the relationship between convective precipitation and column water vapor, Walker-like circulations, self-aggregation of convection, and the Madden–Julian oscillation. The framework is a synthesis of previous work that developed four key approximations: boundary layer energy quasi equilibrium, conservation of free-tropospheric moist and dry static energies, and the weak temperature gradient approximation. It is demonstrated that essential features of slow, convectively coupled processes can be understood without reference to complex turbulent and microphysical processes, even though accounting for such complexity is essential to quantitatively accurate modeling. In particular, we demonstrate that the robust relationship between column water vapor and precipitation observed over tropical oceans does not necessarily imply direct sensitivity of convection to free-tropospheric moisture. We also show that to destabilize the radiative–convective equilibrium state, feedbacks between radiation and clouds and water vapor must be sufficiently strong relative to the gross moist stability.

1. Introduction

Among the most important processes at work in the atmosphere is moist convection, which largely sets the vertical temperature structure of the tropical and parts of the extratropical troposphere and which is an important control on the distribution of clouds and water vapor. Yet it is among the most complex of atmospheric processes, involving detailed microphysical and turbulent physics and poorly understood coupling to the boundary layer and to large-scale atmospheric circulations. Perhaps for this reason, it continues to present serious challenges to numerical weather prediction and climate models, and also to conceptual understanding.

With the advent of global, cloud-permitting models, the need to employ parameterizations of convection diminishes, although for some time it will still be necessary to represent in-cloud turbulence parametrically, and cloud microphysical processes will have to be parameterized indefinitely. Yet even with the increasing use of cloud-permitting models, understanding their behavior (not to mention that of the real world) requires a conceptual framework that provides a qualitatively correct and satisfying view of the underlying mechanisms. Understanding of complex phenomena like the Madden–Julian oscillation (MJO) and self-aggregation of convection will not simply emerge from observations, however comprehensive, or numerical simulations, however successful they might be in replicating the phenomenon.

Aside from being the ultimate objective of the scientific endeavor, understanding is usually an important stepping stone to improving applications. In climate and weather prediction, it is the essential ingredient in, for example, the representation of subgrid-scale processes.

It is in this spirit of conceptual understanding that we here present a candidate conceptual model of slow, convectively coupled processes in the atmosphere. By "slow," we refer specifically to processes whose intrinsic time scale is long compared to time scales associated with internal waves, but nevertheless fast compared to

Denotes content that is immediately available upon publication as open access.

Supplemental information related to this paper is available at the Journals Online website: https://doi.org/10.1175/JAS-D-18-0090.s1.

Corresponding author: Kerry Emanuel, emanuel@mit.edu

DOI: 10.1175/JAS-D-18-0090.1

a pendulum day. (The latter is infinite on the equator, so this second limit is rendered irrelevant.) Under these conditions, the weak temperature gradient (WTG) approximation introduced by Sobel and Bretherton (2000) is satisfied and is a cornerstone of the framework described here. In many respects, the present work follows the pioneering paper of Sobel and Bretherton (2000) and Bretherton and Sobel (2002), but differs in its handling of free-tropospheric moisture and also extends that work to other kinds of circulations, including those driven by unstable interactions among clouds, water vapor, and radiation. But a caveat must be added to the conditions in which WTG is valid: even weak local rotation can lead to small but nonetheless important changes in the character of convection and its associated coupling to larger scales (Raymond et al. 2015), so that the simple framework presented here is probably not appropriate for, for example, the genesis of tropical cyclones.

Three other key assumptions underlie our conceptual model: boundary layer quasi equilibrium, as described by Emanuel (1993) and Raymond (1995); clear-sky energy balance; and the energy balance of the whole troposphere. In addition, we assume that deep convecting regions are nearly neutrally stable to deep convection and that deep convective downdrafts are driven mostly by evaporation of precipitation, whose magnitude in relation to convective updrafts is described by a single precipitation efficiency. We show that the moisture content of the free troposphere in radiative–convective equilibrium (RCE) is determined by this precipitation efficiency, supporting previous work that demonstrates that free-tropospheric moisture is strongly influenced by convective cloud microphysics. As in the work of Bretherton and Sobel (2002), we allow for the dependence of radiative cooling on clouds and water vapor and support, in a conceptually clear way, previous work demonstrating that under some conditions this destabilizes deep convective atmospheres, leading to aggregation of moist convection and explaining such phenomena as the MJO. Even when the cloud and water vapor dependence of radiation is stable, cloud–radiation interactions can substantially concentrate moist convection in forced circulations such as the intertropical convergence zone (ITCZ) and the Walker circulation, as shown by Bretherton and Sobel (2002).

In summary, our intent here is to synthesize the work of many previous investigators into a simple, conceptually clear framework that may help advance future research on slow, convectively coupled processes.

The simple conceptual model is developed in the next section and applied to various slow, convectively coupled processes in successive sections.

2. Simple model framework

The basic framework is illustrated in Fig. 1. Figure 1a is a generic cross section through the tropical atmosphere, showing deep and shallow convection, while characteristic profiles of moist static energy, saturation moist static energy, and large-scale vertical velocity are shown in Fig. 1b. The tropospheric temperature is characterized by its saturation moist static energy h^*, which is constant in height (moist adiabatic temperature profile) and laterally, as well as in time (WTG). In the deep convectively coupled region at the far left in Fig. 1a, the subcloud-layer moist static energy h_b is equal to h^* by the assumption of convective neutrality. As h^* is constant, h_b does not vary laterally and so there can be no horizontal advection of h_b in this region. In Fig. 1a, deep convective updrafts with mass flux M_u transport mass and thermodynamic properties of the subcloud layer upward into the free troposphere, while downdrafts with mass flux M_d carry mass and thermodynamic properties of the lower to middle troposphere downward into the boundary layer. In the clear air outside of cloud systems, air descends with velocity w_e at the top of the boundary layer. Averaged over the ensemble of deep updrafts and downdrafts and clear air, the average (or large scale) vertical velocity at the top of the boundary layer is

$$w = M_u - M_d - w_e. \tag{1}$$

All of these variables may vary slowly in space and time and should be regarded as ensemble averages over the convection. Note that M_d and w_e are defined as positive downward.

As we shall see, if locally the underlying surface enthalpy flux is sufficiently small, deep convection is not supported and the large-scale vertical velocity becomes equal to $-w_e$. In that case, the subcloud layer moist static energy is no longer tied by deep convection to the free-tropospheric h^* and, thus, becomes thermodynamically decoupled, as pointed out, for example, by Bretherton and Sobel (2002). In that case, the subcloud-layer moist static energy must be calculated from the energy balance, and is free to vary horizontally and thus be advected by large-scale flow. This is illustrated on the right side of Fig. 1a.

Conservation of moist static energy[1] in the boundary layer may be written

[1] In reality, moist static energy is not precisely conserved in the atmosphere, and moist entropy is a more nearly conserved variable. But given the level of approximation used in this paper, the nonconservation of moist static energy is a comparatively small effect.

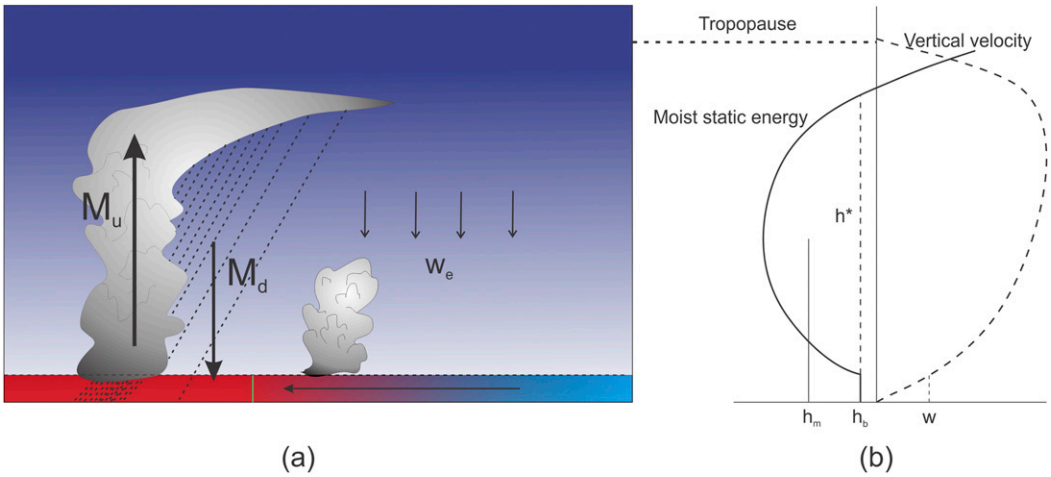

FIG. 1. Illustrating the general conceptual framework for slow, convectively coupled processes. (a) A generic cross section through the tropical atmosphere, showing deep and shallow convection. (b) Characteristic vertical profiles of moist static energy, saturation moist static energy h^* and large-scale vertical velocity are shown. The colors in the subcloud layer represent the magnitude of moist static energy, and the green vertical line separates the deep convectively coupled region at left from the region free of deep convection at right. Deep convective updraft mass fluxes are represented by M_u, downdrafts associated with deep convection by M_d, and the vertical velocity in the clear air by w_e. See text for detailed description.

$$d\left(\frac{\partial h_b}{\partial t} + \mathbf{V}_h \cdot \nabla h_b\right) = F_h - (M_d + w_e)(h_b - h_m) - \dot{Q}_b d, \tag{2}$$

where d is the depth of the boundary layer, h_b is the moist static energy of the boundary layer (which is assumed to be well mixed in the vertical), $\mathbf{V}_h$ is the large-scale horizontal velocity in the boundary layer, F_h is the surface enthalpy flux, h_m is a characteristic value of moist static energy in the free troposphere (see Fig. 1b), and $\dot{Q}_b$ is the radiative cooling of the boundary layer. In writing (2) we have assumed that the moist static energy transported into the boundary layer by deep convective downdrafts has the same value as that entrained into the top of the boundary layer as a consequence of large-scale subsidence. This may not be a good approximation, but we apply it here in the spirit of maximum simplicity.

Boundary layer quasi equilibrium may be thought of as the limit of (2) as the depth d of the boundary layer becomes vanishingly small. In that case, (2) may be approximated, after substituting (1) for the sum $M_d + w_e$, as

$$M_u = w + \frac{F_h}{h_b - h_m}. \tag{3}$$

This is our simple way of dealing with deep moist convection. While relatively crude, it has been used with some success in a forecast model of tropical cyclones (Emanuel and Rappaport 2000) and in models of tropical intraseasonal variability (e.g., Yano and Emanuel 1991). It is important to note that a strong sensitivity of convection to free-tropospheric moisture enters through the denominator of the last term in (3), but this has nothing to do with entrainment into convective clouds. Also note that the convective updraft mass flux diagnosed with (3) is singular in the limit that the air just above the boundary layer becomes saturated. In practice [e.g., in the forecast model discussed in Emanuel and Rappaport (2000)], feedbacks from convection to the moist static energy above the boundary layer usually prevent this from happening.

The representation of convection by (3) is capable of predicting a negative convective mass flux, which is unphysical. In this case we return to (2) and take the mass flux to be zero. Various analyses (e.g., Bretherton and Sobel 2002) show that the lateral advection of moist static energy in the boundary layer cannot be neglected in this case, so that in regions without deep convection, boundary layer quasi equilibrium becomes

$$d\mathbf{V}_h \cdot \nabla h_b \cong F_h - w_e(h_b - h_m) - \dot{Q}_b d. \tag{4}$$

Here, we have retained the radiative cooling of the boundary layer as it can be important when boundary layer clouds are present, as often happens in subsiding regions. Equation (4) should be used wherever (3) predicts a negative mass flux.

As stated above, cloud microphysics are represented by a single precipitation efficiency ϵ_p, which is used to

relate the precipitation-driven downdraft mass flux to the updraft mass flux via

$$M_d = (1 - \epsilon_p) M_u. \tag{5}$$

This is the simplest possible representation that correctly obeys two limits: if convection does not precipitate ($\epsilon_p = 0$), then there is no net release of latent heat over the life cycle of the cloud and there can be no net mass flux ($M_u - M_d = 0$). On the other hand, if all condensate is converted to precipitation and the latter does not evaporate, then the precipitation efficiency is unity and there can be no downdraft. Note that in reality, ϵ_p is a function both of cloud microphysical processes and environmental variables, such as temperature and humidity, that affect rates of evaporation of falling precipitation. In the spirit of maximum simplicity, we hold it constant here.

The WTG approximation requires that the temperature of the free troposphere remains constant in time; nor can there be any lateral advection of temperature. Thus, the dry static energy balance in the clear air, which is presumed to occupy most of the fractional area of the system, is given by

$$w_e S = \dot{Q}, \tag{6}$$

where $\dot{Q}$ is the radiative cooling and S is the dry static stability:

$$S \equiv c_p \frac{dT}{dz} + g, \tag{7}$$

where c_p is the heat capacity and g the acceleration of gravity. Note that both $\dot{Q}$ and S are evaluated just above the top of the boundary layer. Using (1) and (5), (6) becomes

$$(\epsilon_p M_u - w) S = \dot{Q}. \tag{8}$$

Note that in the absence of deep convection, (8) reduces to a simple balance between radiative cooling and subsidence warming.

The final piece of the framework is the conservation of vertically integrated moist static energy in the troposphere. If we take h_m to be the pressure-weighted vertical average of moist static energy in the troposphere, then this conservation relation takes the form

$$H\left(\frac{\partial h_m}{\partial t} + \mathbf{V}_h \cdot \nabla h_m\right) = F_h - \dot{Q}_t H - G_m w, \tag{9}$$

where H is a tropospheric depth scale, $\dot{Q}_t$ is the average radiative cooling of the troposphere, and G_m is the gross moist stability (Neelin and Held 1987), defined

$$G_m \equiv \frac{1}{w} \int_{p_t}^{p_0} \tilde{w} \frac{\partial h_m}{\partial p} dp, \tag{10}$$

in which $\tilde{w}$ is the full vertical profile of the vertical velocity and the limits of integration are the surface and tropopause pressures. Since the profile of the moist static energy h_m has a minimum in the middle troposphere (see Fig. 1b) and since characteristic profiles of $\tilde{w}$ are single signed (Neelin and Yu 1994), the integrand of (10) changes sign and so G_m can be of either sign. In what follows, we assume that the gross moist stability G_m is positive. But we note that as the free troposphere approaches saturation, and assuming that it maintains a moist adiabatic lapse rate, G_m will tend toward zero, so in some of the applications that follow we take G_m to be proportional to $h_b - h_m$.

The horizontal advection of tropospheric moist static energy [second term on the left-hand side of (9)] can be important in the physics of slow convectively coupled processes, as pointed out, for example, by Sobel et al. (2014). But for the present we neglect this term, as it is nonlinear and adds significant complexity to the system; at the same time, we must keep in mind that this is potentially significant.

For simplicity, we also take the average radiative cooling of the troposphere $\dot{Q}_t$ to be equal to the radiative cooling just above the top of the boundary layer $\dot{Q}$.

One interesting feature of (3)–(8) is that these equations only involve quantities evaluated in and just above the boundary layer; they are indifferent to the vertical profiles of convective mass fluxes (and therefore convective entrainment), large-scale vertical velocity, and radiative cooling above the lower troposphere. In essence, our assumption that the troposphere always maintains a moist adiabatic lapse rate implies that the sum of the convective, large-scale adiabatic, and radiative temperature tendencies must always conspire to maintain a moist neutral lapse rate, and the equations are indifferent to which mixture of processes achieves this. On the other hand, the free-tropospheric moisture, controlled by (9), is sensitive to the vertical profiles radiative cooling and of large-scale vertical velocity and moist static energy insofar as they affect the gross moist stability defined by (10). There is no quasi equilibrium of tropospheric moisture, which is sensitive to the details of convection (including microphysics and entrainment) and large-scale advection and radiation. Insofar as these processes influence free-tropospheric moisture, they indirectly influence the cloud-base mass fluxes through the boundary layer quasi-equilibrium closure, (3).

The simple framework can be summarized by using (3) and (8) to solve for M_u and w, and neglecting the horizontal advection term in (9). This results in the following three relations:

$$M_u = \frac{1}{1-\epsilon_p}\left(\frac{F_h}{h_b - h_m} - \frac{\dot{Q}}{S}\right), \tag{11}$$

$$w = \frac{1}{1-\epsilon_p}\left(\frac{\epsilon_p F_h}{h_b - h_m} - \frac{\dot{Q}}{S}\right), \tag{12}$$

and

$$H\frac{\partial h_m}{\partial t} = F_h - \dot{Q}H - G_m w. \tag{13}$$

Note that the entire time dependence of the system is controlled by the single equation for the conservation of tropospheric mean moist static energy. The system is completed by specification of F_h, $\dot{Q}$, G_m, and ϵ_p, possibly as functions of M_u, w, and/or h_m. Note that the convective mass flux and the large-scale vertical velocity both increase with increasing surface enthalpy flux, with decreasing radiative cooling, and with increasing tropospheric moisture as represented by h_m. The magnitudes of the mass flux and vertical velocity also increase with increasing precipitation efficiency. Tropospheric mean moist static energy increases with increasing surface enthalpy flux, decreasing radiative cooling, and decreasing vertical velocity. Also notice that (12) and (13) alone are a complete set, with (11) acting as a diagnostic for the mass flux, unless F_h, $\dot{Q}$, and/or G_m are assumed to be functions of M_u. Finally, note from (8) that in the event that the mass flux vanishes, we must replace (12) by

$$w = \frac{-\dot{Q}}{S}, \tag{14}$$

while (13) remains unchanged and we should add (4) to calculate the boundary layer moist static energy, which becomes a free variable.

This system is in some ways similar to that developed by Bretherton and Sobel (2002), but differs in one essential respect. Both systems use conservation of dry and moist static energies and employ the weak temperature gradient approximation, but Bretherton and Sobel assume a fixed vertical profile of specific humidity, whereas the current system decouples free-tropospheric moisture from the boundary layer and predicts its evolution over time using (13). The extra degree of freedom requires an extra closure relation, provided here by the boundary layer quasi-equilibrium hypothesis.

3. Slow, convectively coupled processes

We next view slow, convectively coupled processes through the lens of the framework developed in the previous section, as expressed by (11)–(14). We begin with the simplest state, radiative–convective equilibrium, and proceed from there.

a. Radiative–convective equilibrium

The RCE state, by definition, is characterized by the absence of any large-scale circulation, and is statistically steady, so we set $w = 0$. The steady form of (13) is just

$$F_h = \dot{Q}H. \tag{15}$$

It follows from (12) that

$$\frac{h_b - h_m}{SH} = \epsilon_p. \tag{16}$$

Since $h_b = h^*$ and the latter is constant through the troposphere, $h_b - h_m = h^* - h_m = L_v q_m^*(1-\mathcal{H})$, where L_v is the latent heat of vaporization, q_m^* is the saturation specific humidity of the middle troposphere, and $\mathcal{H}$ is the relative humidity. Since SH also scales with saturation specific humidity, (16) becomes approximately

$$\mathcal{H} \approx 1 - \epsilon_p. \tag{17}$$

The relative humidity of the troposphere is controlled largely by cloud microphysical properties, as represented here by a single precipitation efficiency. More efficient rain-out leads to a drier troposphere, while low precipitation efficiency will lead to greater relative humidity. This is consistent with previous work (e.g., Emanuel 1991; Emanuel and Pierrehumbert 1996; Emanuel and Živkovic-Rothman 1999) that demonstrated the sensitivity of atmospheric water vapor to cloud microphysics.

Setting $w = 0$ in (8) shows that in RCE

$$M_u = \frac{\dot{Q}}{S\epsilon_p}. \tag{18}$$

The convective updraft mass flux is also sensitive to cloud microphysics as represented by ϵ_p. Another inference is that greenhouse gas–induced warming, which increases radiative cooling but increases dry static stability along a moist adiabat (which scales with the saturation specific humidity) faster, leads to a decrease in convective mass flux (Held and Soden 2006). Since, in RCE, precipitation increases with radiative cooling, decreasing convective mass flux paired with increasing

precipitation implies increased intensity of precipitation: greater rainfall rates where and when it is raining, and longer intervals between rain events. This is consistent with the behavior of global climate models described by Held and Soden (2006), and while the argument presented here is not identical to theirs, it is consistent with it.

b. Response to forced changes in surface enthalpy flux

We next examine the response of the tropical atmosphere to specified perturbations in the surface enthalpy flux. For the purpose of this endeavor, we hold the precipitation efficiency ϵ_p fixed but allow the radiative cooling $\dot{Q}$ and the gross moist stability G_m potentially to vary. For convenience of notation, we replace the dimensional variables, parameters, and time by scaled equivalents, as follows:

$$M_u = \frac{Q_0}{S\epsilon_p(1-\epsilon_p)} M, \tag{19}$$

$$w = \frac{Q_0}{S(1-\epsilon_p)} W, \tag{20}$$

$$h_b - h_m = \epsilon_p SH(1+D), \tag{21}$$

$$F_h = Q_0 H(1+F), \tag{22}$$

$$G_m = HS(1-\epsilon_p)G, \tag{23}$$

$$\dot{Q} = Q_0(1+Q), \tag{24}$$

and

$$t = \frac{SH}{Q_0}\tau. \tag{25}$$

Here, Q_0 is the RCE state radiative cooling, Q is the nondimensional departure from that RCE state, D is a nondimensional measure of the dryness of the free troposphere relative to the RCE state, and F is the nondimensional departure of the surface enthalpy flux from the RCE state. (These departures need not be small. Also, note that saturation is achieved when $D = -1$.) The time scale t in (25) is the time for clear air to descend through the troposphere under the influence of radiative cooling; this is on the order of 2 weeks and defines what we mean by "slow." Remember that under the WTG approximation, h_b and S are invariant in space and time.

With the substitutions of (19)–(25), the set (11)–(13) becomes

$$M = \frac{1+F}{1+D} - \epsilon_p(1+Q), \tag{26}$$

$$W = \frac{1+F}{1+D} - (1+Q), \tag{27}$$

and

$$\frac{\partial D}{\partial \tau} = Q - F + GW. \tag{28}$$

By eliminating W between (27) and (28), we obtain

$$\frac{\partial D}{\partial \tau} = Q(1-G) - F + G\frac{F-D}{1+D}. \tag{29}$$

A first observation about (29) is that if there are no perturbations to radiative cooling or surface fluxes that are tied to other variables like moisture ($Q = F = 0$), (29) reduces to

$$\frac{\partial D}{\partial \tau} = -G\frac{D}{1+D}.$$

For positive gross moist stability, this is always stable, even if we let $G \approx 1 + D$ so that the gross moist stability gets larger as the troposphere gets drier and vanishes if the troposphere is saturated. Therefore, in the absence of variations in radiative cooling and surface enthalpy fluxes, the RCE state is stable in this model. Thus, we are entitled to look for steady solutions for invariant radiation ($Q = 0$) and fixed, specified surface enthalpy flux F by setting the time derivative in (29) to zero and finding M, W, and D as functions of F:

$$M = \frac{F}{G} + 1 - \epsilon_p, \tag{30}$$

$$W = \frac{F}{G}, \tag{31}$$

and

$$D = \frac{-F(1-G)}{F+G}. \tag{32}$$

In regions where (30) predicts a nonpositive value of M, we set $M = 0$ and replace (31) by

$$W = -(1-\epsilon_p). \tag{33}$$

Note that the value of D is indeterminate in this case, and we could, if we wished, solve the nondimensional equivalent of (4) for the boundary layer moist static energy, given a horizontal velocity and a value for h_m.

The form of (32) shows that no matter how large the surface fluxes become, the troposphere never saturates; that is, $D > -1$. On the other hand, the mass flux increases indefinitely with F. The solutions for (30), (31), and (33) are plotted as a function of F in Fig. 2a, for

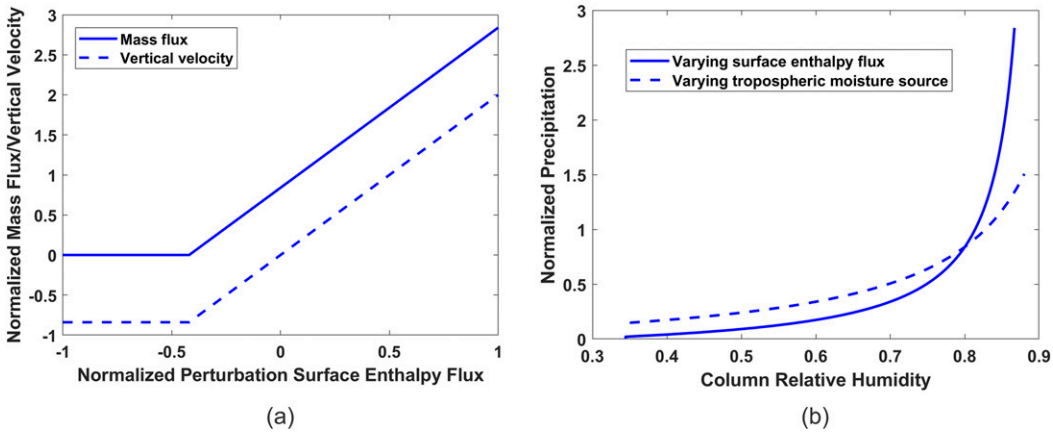

FIG. 2. (a) The normalized convective updraft mass flux (solid) and large-scale vertical velocity (dashed) are plotted against the specified normalized perturbation of the surface enthalpy flux. (b) The normalized precipitation is plotted against the column relative humidity. The dashed curve in (b) shows the response to injecting water vapor into the free troposphere while holding surface fluxes constant.

$\epsilon_p = 0.25$ and $G = 0.5$. The updraft mass flux and large-scale vertical velocity are simply linear functions of the perturbation surface enthalpy flux down to a critical value, below which the deep convective mass flux vanishes and the large-scale descent just balances the (prescribed) radiative cooling. In Fig. 2b, the normalized precipitation rate (which in this normalization[2] is just proportional to $\epsilon_p M$) is plotted against the column relative humidity rather than against F. Here, the column relative humidity is approximated via (21) as $1 - 0.2(1 + D)$, so that it is 80% in RCE. In this case, since we have no way of calculating D when $M = 0$, we set it, over the whole range of F for which $M = 0$, to its smallest value in the convecting region. Thus, the last point on the left of Fig. 2b represents the whole region of no deep convection. The precipitation increases quite nonlinearly with column moisture, as first noted by Raymond and Zeng (2000) and Bretherton et al. (2004) and subsequently investigated by many others (e.g., Peters and Neelin 2006; Neelin et al. 2009; Kuo et al. 2017). (In fact, since M increases indefinitely with F while D approaches a limiting value, the curve asymptotically becomes vertical.) The most common interpretation of this apparent dependence of convection on column moisture is that convection is suppressed through entrainment of dry environmental air (e.g., Kuo et al. 2017). But within the current framework, entrainment is not accounted for except that it influences the value of G. Yet examination of (11) shows that the convective mass flux responds directly to increasing surface fluxes and also to free-tropospheric moisture through the term in the denominator. In essence, a drier free troposphere requires less convective updraft mass flux to produce the same downdraft flux of low moist static energy into the boundary layer, needed to balance surface fluxes. This has nothing to do with convective entrainment. The solid curve in Fig. 2b results both from the direct response of convection to increasing surface fluxes and to the resulting moistening of the free troposphere.

We can isolate the effect of midtropospheric moisture by injecting water vapor directly into the free troposphere (say, by horizontal advection or a horizontal eddy flux) while holding the surface flux constant. This can be accomplished by setting $Q = F = 0$ in (26) and (29) and adding a specified source to the right-hand side of (29), allowing it to vary over a specified range. The result, graphing precipitation against column water vapor, is shown by the dashed line in Fig. 2b. Injecting water into the free troposphere does indeed increase precipitation, but considerably more slowly than increasing surface fluxes (which also moistens the free troposphere but contributes directly to the increase in precipitation as well).

In the online supplemental information, we consider two variants on the model described in this section. In the first, the gross moist stability G is replaced by $G(1 + D)$. This has the effect of letting the gross moist stability vanish when the atmosphere is saturated, and so the integral (10) vanishes along a moist adiabat. Conversely, the gross moist stability increases in an atmosphere that is drier than RCE. Figure S1 shows the results, which are also compared to the standard results

[2] But note that variations in boundary layer moisture are not accounted for in this estimate of normalized precipitation; in effect, the boundary layer moisture is part of the normalization.

shown in Fig. 2. The second variant retains the original, constant G but allows the radiative cooling to diminish with updraft mass flux: $Q = -\alpha(M - M_{\mathrm{eq}})$, where α is a constant and M_{eq} is the mass flux in RCE. This is very similar to the representation of cloud-radiative effects used by Bretherton and Sobel (2002). Figure S2 compares solutions of this system to the control shown in Fig. 2. Both modifications have the effect of amplifying the dependence of the mass flux on surface forcing and allowing the troposphere to become more humid in response to the forcing.

c. Walker circulations

For variations in the surface enthalpy flux F that are not strong enough to cause the cumulus updraft mass flux M to vanish anywhere, the relations (26), (27), and (29) are valid in every column independently of other columns, and at first blush there appears to be no mechanism by which columns may "talk" to one another. Yet if we take some equatorial region bounded by vertical walls at its eastern and western extremities, then we must insist that there be no net large-scale vertical mass flux integrated across the domain. If we apply (31) in each column, the requirement that the domain average vertical velocity vanish is equivalent to requiring that the domain average perturbation surface flux vanishes.

In reality, as pointed out by Bretherton and Sobel (2002), this is accomplished by an adjustment of the free-tropospheric temperature. Although for the present purpose we are specifying the surface enthalpy flux, in reality it conforms to an aerodynamic flux formula of the form

$$F_h = C_k|\mathbf{V}|(h_0^* - h_b) = C_k|\mathbf{V}|(h_0^* - h^*), \tag{34}$$

where C_k is a dimensionless surface exchange coefficient, $|\mathbf{V}|$ is a near-surface wind speed, and h_0^* is the moist static energy at saturation at sea surface pressure and temperature. The second equality in (34) arises owing to the assumption of deep convective neutrality, $h_b = h^*$, in convectively coupled regions. In a less simple formulation than the present one, we would specify the surface temperature (equivalent to specifying h_0^*) and perhaps the wind speed, but h^*, assumed constant in time in this problem, would remain a free parameter and will adjust itself to ensure that there is no net upward motion averaged over the domain.

As an example, we take

$$F = -A\tanh(x), \qquad -3 \le x \le 3, \tag{35}$$

where A is an amplitude factor and x is some normalized zonal scale. (Note that it does not matter, in this system, how x is normalized, but if the scale of variation of F is too large, the approximations underlying the weak temperature gradient approximation may break down, and if it is too small, then the assumption that we are dealing with ensemble averages of cumulus clouds will fail.) This is consistent with a warm ocean in the west and a cold ocean in the east. Substituting (35) into (30), we see that M will not vanish anywhere provided

$$A < G\frac{1-\epsilon_p}{\tanh(3)}. \tag{36}$$

In this case, the cumulus mass flux and large-scale vertical velocity would just vary as $\tanh(x)$, according to (30) and (31), and the relationship between the column humidity and precipitation would be that shown in Fig. 2.

But now suppose the amplitude is large enough to violate the condition (36). In that case, M will vanish over some span of the right side of the domain, and where this happens, the vertical velocity is given by (33). But in such regions, the boundary layer moist static energy h_b is decoupled from the free troposphere and to find the dividing longitude between a deep convectively coupled regime in the west, and a shallow convection regime in the east, we have to find out where the boundary layer moist static energy first becomes large enough to convect as one moves from east to west, as can be visualized with the aid of Fig. 1.

Here, we have to employ the conservation equation for boundary layer moist static energy, (4), which in this case is

$$du\frac{\partial h_b}{\partial x} = F_h + w(h_b - h_m), \tag{37}$$

where u is the zonal velocity. But from mass continuity,

$$du = -\int_x^3 w\,dx = w(3-x), \tag{38}$$

where for the last equality we have made use of the fact the w is constant in the convectively uncoupled domain and take the eastern boundary to lie at $x = 3$.

Without deep convection, there is no constraint on the value of h_m and absent lateral advection, it would become quite small under the influence of subsidence and radiative cooling. Lateral advection and mixing would usually serve to keep its value elevated over such a bare minimum. Here, for simplicity, we take h_m to be constant and equal to its (computed) value at the far eastern side of the convectively coupled region, as though lateral mixing from west to east were perfectly efficient.

Thus, we take h_m as being constant in (37), use the normalization for F given by (22), take $w = -Q_0/S$ from (14), and introduce a normalized boundary layer moist static energy surplus D_b:

$$h_b - h_m \equiv SHD_b. \tag{39}$$

Using these relations and (38), (37) becomes

$$(3-x)\frac{\partial D_b}{\partial x} - D_b = -1 - F. \tag{40}$$

We next use (35) to specify the surface enthalpy flux, but add a constant offset F_0, which we will discuss later. The solution to (40) is then

$$D_b = 1 + F_0 + \frac{A}{3-x}\ln\left[\frac{\cosh(x)}{\cosh(3)}\right]. \tag{41}$$

As we move from the eastern boundary at $x = 3$ westward, the boundary layer moist static energy, as represented by D_b, increases. It will become high enough for deep convective neutrality when the value of $h_b - h_m$ becomes equal to that of the easternmost convectively coupled region, given that we are holding h_m constant from there across the decoupled region. Comparing the normalizations (39) and (21), we see that this happens when

$$D_b = \epsilon_p(1 + D). \tag{42}$$

This condition determines the value of x separating the deep convecting region to the west from the decoupled region to the east. The solution in the convectively coupled region is given once again by (30)–(32), except that we add the same constant, F_0, to the perturbation surface enthalpy flux.

Calculating this solution with a trial value of F_0 and then taking the domain average of W, we will find it is nonzero. Accordingly, we adjust the value of F_0 iteratively until the domain average of $|W|$ is sufficiently small.

As before, we consider two variants of this system. The first replaces G with $G(1 + D)$ so that the gross moist stability vanishes in a saturated troposphere. In this case, we use (S1)–(S3) in the online supplement in place of (30)–(32). In the second case, we take $Q = -\alpha M$ to mimic cloud-radiative feedbacks. (Note that the RCE solution differs from the control in this case; we implement this so that the clear-sky cooling in the uncoupled region has the same value as in the control and variable G experiments.) In this case we replace (30)–(32) in the convectively coupled region with (S12)–(S14) from the supplemental material.

Solutions for the convective updraft mass flux and boundary layer moist static energy surplus are shown in Fig. 3. The latter quantity is defined as $(h_b - h_m)/SH$. In the convectively coupled region, this varies slightly owing to variations of h_m (since $h_b = h^* =$ constant in this region) while its variations in the decoupled region are exclusively owing to variations in h_b as h_m is fixed in this region. The calculations are done for $G = 0.5$, $\epsilon_p = 0.25$, and, in the case of cloud-radiative feedback, $\alpha = 0.5$. For comparison, the variation in convective mass flux in the absence of horizontal advection of boundary layer moist static energy is shown by the light blue curve in Fig. 3. Boundary layer moist static energy advection strongly displaces the deep convecting zone westward by stabilizing the boundary layer where there are strong zonal gradients of the surface enthalpy flux, and causes the mass flux to end abruptly on its eastern flank. Allowing the gross moist stability to decrease with increasing tropospheric humidity acts as a strong positive feedback, further amplifying and concentrating the convection in the far western portion of the domain. Feedback between clouds and radiation also acts to concentrate and amplify the convective mass flux. Taken together, these results are very similar to those of Bretherton and Sobel (2002), with the added conclusion that variability of the gross moist stability has a substantial influence on the solution.

d. *Concentration of the intertropical convergence zone*

For zonally invariant circulations near the equator, the zonal component of the flow is likely to be rotationally constrained even fairly close to the equator, and the temperature above the boundary layer cannot so easily be assumed to be constant in latitude. Nevertheless, if the flow is assumed to be steady, then (11), (12), and the steady form of (13) still hold although the boundary layer moist static energy h_b and the dry static stability S can no longer be assumed to be constant in deep, convectively coupled regions. But fractional changes in S should be small sufficiently near the equator and so we continue to approximate it as a constant. In applying the variable transformation, (21), we must now regard D as including the variability of h_b as well as that of h_m. Otherwise, the system is identical to that we considered in the previous section on the Walker circulation, except that the spatial coordinate is latitude rather than longitude, and the meridional wind v, rather than the zonal wind u, is calculated from mass continuity.

At first blush, it seems as if we have circumvented the whole issue of rotational constraints on the Hadley circulation, of the kind considered by Held and Hou (1980).

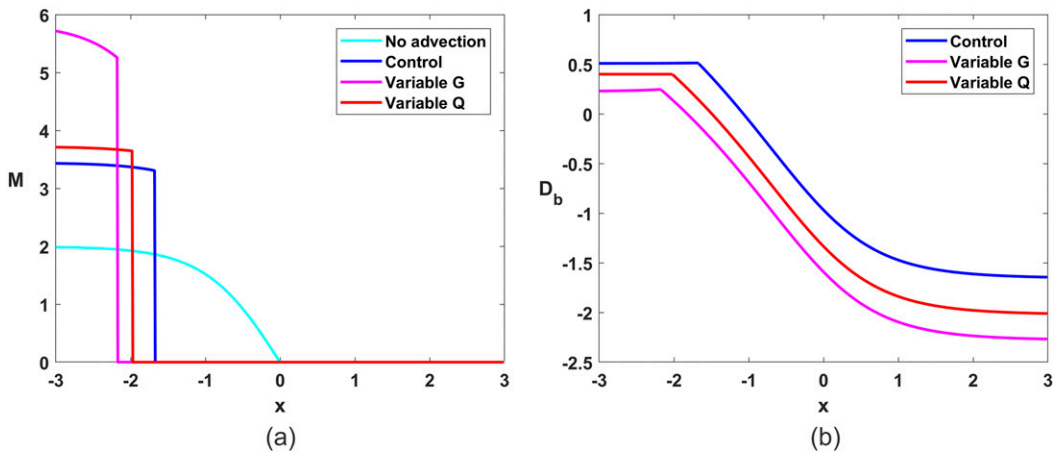

FIG. 3. Solutions for (a) convective updraft mass flux and (b) normalized difference between boundary layer and midtropospheric most static energy as a function of zonal distance x for the Walker circulation model. The dark blue curves are for the control experiment, while the magenta and red curves are for experiments with a moisture-dependent gross moist stability and a convection-dependent radiative cooling, respectively. The light blue in (a) is for an experiment omitting horizontal advection of boundary layer moist static energy.

Indeed, we have done so, through the artifice of specifying the surface enthalpy flux, rather than, say, specifying the surface temperature and calculating the flux interactively. To see this, suppose that the surface temperature varies slowly enough with latitude so as not to violate the Held–Hou condition (Held and Hou 1980) that the angular momentum associated with the thermal wind solution must decrease monotonically away from the equator. [See also Emanuel (1995).] Then each column, in latitude, can be individually in radiative–convective equilibrium, with the resulting horizontal temperature gradient balanced by Coriolis accelerations acting on the zonal wind. In this case, the surface enthalpy flux would balance the radiative cooling at each latitude; if the radiative cooling were constant, then there would be no perturbation in the surface enthalpy flux ($F = 0$ in our notation). By specifying the surface enthalpy flux, we remove that degree of freedom and thus do violence to the Held–Hou condition. Thus, for consistency, we assume that that condition is indeed violated. Our purpose here is not to develop a closed model of the Hadley circulation but to examine conditions under which the ITCZ becomes concentrated.

With this in mind, we specify the surface flux according to

$$F = Ae^{-by^2}, \tag{43}$$

where A is an amplitude and b governs the rate at which the flux decreases away from the equator. As before, we add a constant F_0 to this flux and adjust it to achieve zero average vertical velocity over the domain in y, and we also hold h_m to be constant in the uncoupled region. The equivalent of (40) is then

$$y\frac{dD_b}{dy} + D_b = 1 + F_0 + Ae^{-by^2}, \tag{44}$$

the solution of which, obeying symmetry about the equator, is

$$D_b = 1 + F_0 + \frac{A}{2}\sqrt{\frac{\pi}{b}}\,\frac{\mathrm{erf}(\sqrt{b}\,y)}{y}. \tag{45}$$

Note that this is not singular at the equator, because the error function also vanishes there; the last factor on the right-hand side of (45) takes on the value A in the limit $y \to 0$.

Solutions for the convective updraft mass flux M are compared to the specified distribution of surface fluxes in Fig. 4. The calculations used to create Fig. 4 figure take $G = 0.5$, $\epsilon_p = 0.25$, $A = 1$, $b = 0.5$, and, in the case of cloud–radiative feedback, $\alpha = 0.5$. Horizontal advection causes convection to end abruptly at its north and south extremities, and cloud–radiation feedback further concentrates the convection, as does allowing the gross moist stability to depend on tropospheric moisture (not shown).

e. *Instability of the RCE state and self-aggregation of convection*

Under some circumstances, RCE convection simulated in cloud-permitting models collapses into one or a small number of clusters [see the review by Wing et al. (2017)].

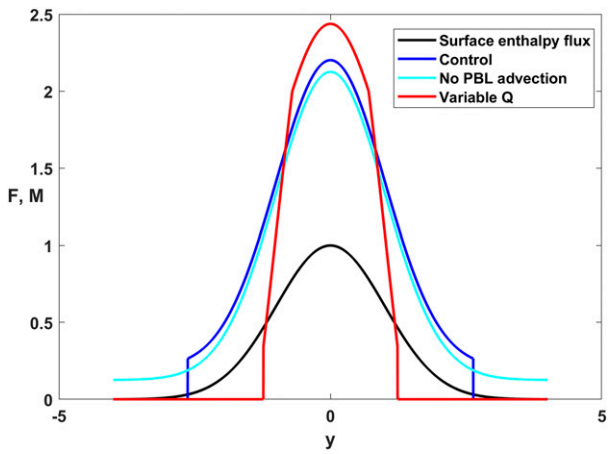

FIG. 4. Application to the ITCZ: specified distribution of normalized surface enthalpy flux (black) compared to calculated distributions of convective updraft mass fluxes M for the control experiment (dark blue), an experiment in which horizontal advection of boundary layer moist static energy is omitted (light blue), and an experiment including a representation of the cloud–radiative feedback (red).

In nonrotating simulations, feedbacks between radiative cooling and clouds and/or water vapor are essential, as first demonstrated by Bretherton et al. (2005), and feedbacks between convection and surface fluxes can also aid the instability (Wing and Emanuel 2014). Here, we examine the conditions under which RCE convection is unstable within our simple framework if we allow the radiative cooling to depend on the convective mass flux.

We examine the growth or decay of small perturbations to the RCE state. In reality, changing the convective mass flux and changing the free-tropospheric moisture can change the surface fluxes through their effects on surface wind gustiness (Wing and Emanuel 2014) and on the thermodynamic properties of downdrafts, but, in keeping with the spirit of simplicity, we take $F = 0$ in (29),

$$\frac{\partial D}{\partial \tau} = Q(1-G) - \frac{GD}{1+D}, \tag{46}$$

and allowing the perturbation radiative cooling, as before, to vary as the convective updraft mass flux via $Q = -\alpha(M - M_{\mathrm{eq}})$, where α is a constant governing the magnitude of the cloud–radiative feedback, subject to the condition that $Q > -1$ so that there is no ascent in the clear air. Using $M_{\mathrm{eq}} = 1 - \epsilon_p$ and (26), with $F = 0$, for M gives

$$Q = \max\left[\frac{\alpha D}{(1+D)(1-\alpha\epsilon_p)}, -1\right]. \tag{47}$$

Thus, (46) and (47) constitute a closed system. For D large enough not to come up against the cap in radiative cooling in (47), combining (46) and (47) gives

$$\frac{\partial D}{\partial \tau} = \frac{D}{1+D}\left[\frac{\alpha(1-G)}{1-\alpha\epsilon_p} - G\right] \quad \text{for} \quad Q > -1, \tag{48}$$

so that the criterion for instability is

$$\alpha > \frac{G}{1 - G(1-\epsilon_p)}. \tag{49}$$

The RCE state is unstable for sufficiently strong cloud–radiative feedback, and this criterion is more easily met for smaller values of the gross moist stability G and for larger values of the precipitation efficiency ϵ_p. In the event that the negative value of D is small enough to come up to the cap in (47), then $Q = -1$ and (46) becomes

$$\frac{\partial D}{\partial \tau} = -(1-G) - \frac{GD}{1+D} \quad \text{for} \quad Q = -1. \tag{50}$$

Both (48) and (50) have analytic nonlinear solutions, which can be expressed explicitly in terms of time as a function of D:

$$\tau = \frac{1}{\mu}\left[\log\left(\frac{D}{D_0}\right) + D - D_0\right] \quad \text{for} \quad Q > -1,$$

$$\tau = \tau_Q + G\log\left(\frac{D_Q + 1 - G}{D + 1 - G}\right) + D_Q - D \quad \text{for} \quad Q = -1, \tag{51}$$

where

$$\mu \equiv \frac{\alpha(1-G)}{1-\alpha\epsilon_p} - G \tag{52}$$

and is positive for growing disturbances. The quantities τ_Q and D_Q are the values of time and D at which Q based on the top part of (51) first becomes as small as -1. This critical value of D from (47) is

$$D_Q = \frac{-1}{1 + \dfrac{\alpha}{1-\alpha\epsilon_p}}, \tag{53}$$

while t_Q is the solution to the top part of (51) using this critical value of D. Note that in the bottom part of (51), time approaches infinity as $D \to -(1+G)$, so that at large time the system asymptotically approaches a steady state.

The corresponding solutions for M, from (26) and using (47), are

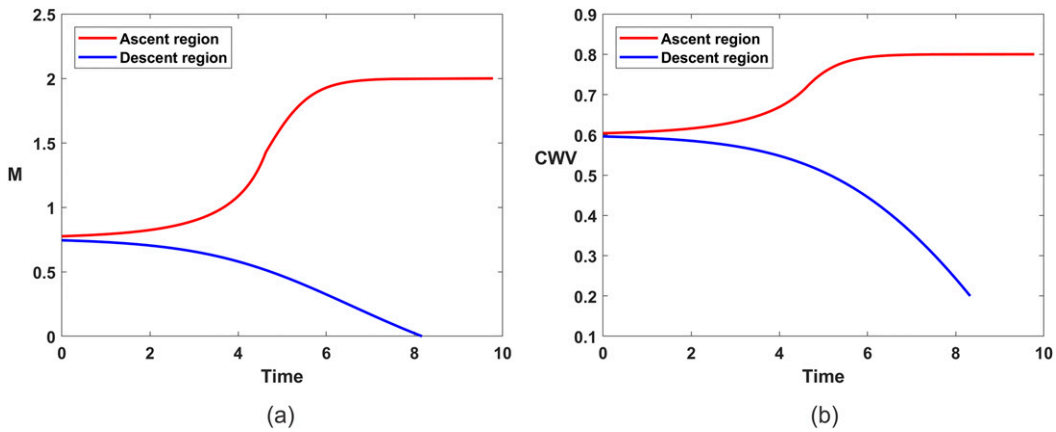

FIG. 5. (a) Nondimensional cumulus updraft mass flux and (b) a measure of column relative humidity for the particular combination of model parameters discussed in the text.

$$M = 1 - \epsilon_p - \frac{D}{(1+D)(1-\alpha\epsilon_p)} \quad \text{for} \quad Q > -1,$$

$$M = \frac{1}{1+D} \quad \text{for} \quad Q = -1. \tag{54}$$

Values of W may be found using (27) with $F = 0$ and using (47) for Q.

From the top part of (54) it can be seen that M vanishes when $D \equiv D_{\max} = a/(1-a)$, where $a \equiv (1-\epsilon_p)(1-\alpha\epsilon_p)$. Thus, for growing solutions D spans the range between $-(1-G)$ and $D_{\max}$. For times beyond the time when $D = D_{\max}$ the descending region becomes convectively uncoupled and control on the value of D there is lost.

An example of these solutions, using (51)–(54), is shown in Fig. 5, for $G = 0.5$, $\epsilon_p = 0.25$, and $\alpha = 1.5$. Initially, negative and positive perturbations amplify at the same rate but after they become sufficiently large, the upward motion intensifies more rapidly than does the descent. The same is true of the large-scale vertical velocity. The final magnitude of the upward motion is larger than that of the descent, but not by much. For the simulation shown in Fig. 5, the implied fractional area of the steady-state large-scale ascent is about 45%.

f. RCE instability with WISHE

As a final illustration of the utility of this simple framework for understanding slow convectively coupled tropical disturbances, we add one further ingredient to the RCE instability problem considered in the previous subsection: the influence of wind-induced fluctuations in the surface enthalpy flux [wind-induced surface heat exchange (WISHE)]. If we linearize the surface enthalpy flux given by (34) about a mean zonal flow of magnitude $\overline{U}$, the result is

$$F'_h = C_k(h_0^* - h^*)\mathrm{sign}(\overline{U})u', \tag{55}$$

where u' is the fluctuating component of the zonal wind. Here, we will confine ourselves to linear disturbances that vary only in the zonal direction, and relate the zonal wind to the vertical velocity using the Boussinesq form of mass continuity in two dimensions:

$$\frac{\partial u'}{\partial x} = -\frac{\partial w'}{\partial z} \simeq -\frac{w'}{H}. \tag{56}$$

Hereafter, we take $\mathrm{sign}(\overline{U}) = -1$ in (55), assuming that the background flow is from the east, as is usually the case in the tropics. To the normalizations, (19)–(25), we add

$$u' \to |\overline{U}|U' \tag{57}$$

and

$$x \to H\frac{SH\epsilon_p(1-\epsilon_p)}{C_k(h_0^* - h^*)}X. \tag{58}$$

For typical values of the parameters, the zonal velocity scale is 5–10 m s^{-1} and the zonal length scale is a few thousand kilometers. The relations (55) and (56) then become simply

$$F' = -U' \tag{59}$$

and

$$\frac{\partial U'}{\partial X} = -W'. \tag{60}$$

We next combine these with the linearizations of (26)–(28) about the RCE state, using the same formulation of radiation as in the previous subsection ($Q' = -\alpha M'$):

$$M' = F' - D' + \epsilon_p \alpha M', \tag{61}$$

$$W' = F' - D' + \alpha M', \tag{62}$$

and

$$\frac{\partial D'}{\partial \tau} = -\alpha M' - F' + GW'. \tag{63}$$

The linear system then consists of (59)–(63). We look for modal solutions of the form $e^{ikX+\sigma\tau}$, which substituted into (59)–(63) gives an equation for the complex growth rate σ. Defining

$$\alpha' \equiv \frac{\alpha}{1-\epsilon_p \alpha} \quad \text{and} \quad k' = \frac{k}{1+\alpha'}, \tag{64}$$

this equation for the complex growth rate is

$$\sigma = -1 + (1+\alpha')(1-G)\frac{k'^2 - ik'}{1+k'^2}. \tag{65}$$

Note that when $k' = 0$, $\sigma = -1$ and so the perturbations decay with time. Conversely, when $k' \to \infty$ the growth rate approaches $\alpha'(1-G) - G$, and the criterion for instability [taking into account the definitions in (64)] is equivalent to (49). In general, the real part of the growth rate σ_r, and the phase speed of the disturbances are given by

$$\sigma_r = -1 + (1+\alpha')(1-G)\frac{k'^2}{1+k'^2} \quad \text{and} \tag{66}$$

$$c = -\frac{\sigma_i}{k} = \frac{(1+\alpha')(1-G)}{1+k'^2}. \tag{67}$$

From (66) it is readily apparent that growing solutions are only possible for $G < \alpha'/(1+\alpha')$, and that the most rapidly growing modes have large zonal wavenumbers, though other processes such as wave radiation into the stratosphere (Yano and Emanuel 1991) or small convective time lags (Emanuel 1993) might limit the size of the wavenumber. The growth rates are on the slow time scale, governed by how rapidly radiation and surface fluxes can change the mean moist static energy of the troposphere. The phase speed is always eastward (against the mean flow) and its largest magnitude also corresponds to a high zonal wavenumber. Considering the scaling for x given by (58) and that for time given by (25), the dimensional phase speed scales with $|\overline{U}|(1-\epsilon_p)$, which is comparable to the mean flow magnitude $|\overline{U}|$, so these are slowly propagating disturbances.

Thus, WISHE actually diminishes the growth rate of the slow disturbances destabilized by cloud–radiation interactions, but causes them to propagate slowly against the mean flow. When placed on an equatorial beta plane, we expect these characteristics to remain qualitatively unchanged, and perhaps to provide a simple framework for the Madden–Julian oscillation (MJO), consistent with the results of Fuchs and Raymond (2005), who argued that the MJO is driven by cloud–radiation interactions but propagates eastward owing to WISHE, and also with Arnold and Randall (2015), who, consistent with Fuchs and Raymond, showed that the MJO in a global model with constant fixed sea surface temperature is driven by the interaction of radiation with clouds and water vapor. But it is not clear that the weak temperature gradient formalism used here is appropriate for the MJO; this issue is explored in Fuchs and Raymond (2017) and Khairoutdinov and Emanuel (2018).

4. Summary

By combining the principles of boundary layer quasi equilibrium and the weak temperature gradient approximation (WTG) with conservation of dry and moist static energy, we have arrived at a simple framework for exploring and understanding slow, convectively coupled processes in the tropical atmosphere. Here, "slow" denotes a time scale associated with adjustments of column-integrated moist static energy and can be thought of as the time scale over which surface enthalpy fluxes and radiation change the column moist static energy. Although very simple, this framework potentially explains such features of the tropical atmosphere as the dependence of humidity on precipitation efficiency, the rapid increase of precipitation with column water, the concentration of the region of upward motion in the Walker and Hadley circulations, and circulations driven by cloud–radiation interaction, such as self-aggregation of convection and the MJO. In future work we will relax the WTG approximation and explore slow circulations influenced by rotation, which can be important even for small-scale systems such as nascent tropical cyclones (Raymond et al. 2015).

Acknowledgments. The author thanks David Raymond and Chris Holloway for very helpful suggestions. This work was supported by the National Science Foundation under Grant AGS-1461517.

REFERENCES

Arnold, N. P., and D. A. Randall, 2015: Global-scale convective aggregation: Implications for the Madden–Julian oscillation. *J. Adv. Model. Earth Syst.*, **7**, 1499–1518, https://doi.org/10.1002/2015MS000498.

Bretherton, C. S., and A. H. Sobel, 2002: A simple model of a convectively coupled Walker circulation using the weak temperature gradient approximation. *J. Climate*, **15**, 2907–2920, https://doi.org/10.1175/1520-0442(2002)015<2907:ASMOAC>2.0.CO;2.

——, M. E. Peters, and L. E. Back, 2004: Relationships between water vapor path and precipitation over the tropical oceans. *J. Climate*, **17**, 1517–1528, https://doi.org/10.1175/1520-0442(2004)017<1517:RBWVPA>2.0.CO;2.

——, P. N. Blossey, and M. F. Khairoutdinov, 2005: An energy-balance analysis of deep convective self-aggregation above uniform SST. *J. Atmos. Sci.*, **62**, 4273–4292, https://doi.org/10.1175/JAS3614.1.

Emanuel, K. A., 1991: A scheme for representing cumulus convection in large-scale models. *J. Atmos. Sci.*, **48**, 2313–2335, https://doi.org/10.1175/1520-0469(1991)048<2313:ASFRCC>2.0.CO;2.

——, 1993: The effect of convective response time on WISHE modes. *J. Atmos. Sci.*, **50**, 1763–1775, https://doi.org/10.1175/1520-0469(1993)050<1763:TEOCRT>2.0.CO;2.

——, 1995: On thermally direct circulations in moist atmospheres. *J. Atmos. Sci.*, **52**, 1529–1534, https://doi.org/10.1175/1520-0469(1995)052<1529:OTDCIM>2.0.CO;2.

——, and R. T. Pierrehumbert, 1996: Microphysical and dynamical control of tropospheric water vapor. *Clouds, Chemistry and Climate*, P. J. Crutzen and V. Ramanathan, Eds., Springer-Verlag, 17–28, https://doi.org/10.1007/978-3-642-61051-6_2.

——, and M. Živkovic-Rothman, 1999: Development and evaluation of a convection scheme for use in climate models. *J. Atmos. Sci.*, **56**, 1766–1782, https://doi.org/10.1175/1520-0469(1999)056<1766:DAEOAC>2.0.CO;2.

——, and E. Rappaport, 2000: Forecast skill of a simplified hurricane intensity prediction model. Preprints, *24th Conf. on Hurricanes and Tropical Meteorology*, Fort Lauderdale, FL, Amer. Meteor. Soc., 236–237.

Fuchs, Z., and D. J. Raymond, 2005: Large-scale modes in a rotating atmosphere with radiative–convective instability and WISHE. *J. Atmos. Sci.*, **62**, 4084–4094, https://doi.org/10.1175/JAS3582.1.

——, and ——, 2017: A simple model of intraseasonal oscillations. *J. Adv. Model. Earth Syst.*, **9**, 1195–1211, https://doi.org/10.1002/2017MS000963.

Held, I. M., and A. Y. Hou, 1980: Nonlinear axially symmetric circulations in a nearly inviscid atmosphere. *J. Atmos. Sci.*, **37**, 515–533, https://doi.org/10.1175/1520-0469(1980)037<0515:NASCIA>2.0.CO;2.

——, and B. J. Soden, 2006: Robust response of the hydrological cycle to global warming. *J. Climate*, **19**, 5686–5699, https://doi.org/10.1175/JCLI3990.1.

Khairoutdinov, M. F., and K. Emanuel, 2018: Intraseasonal variability in a cloud-permitting near-global equatorial aquaplanet model. *J. Atmos. Sci.*, **75**, 4337–4355, https://doi.org/10.1175/JAS-D-18-0152.1.

Kuo, Y.-H., D. J. Neelin, and C. R. Mechoso, 2017: Tropical convective transition statistics and causality in the water vapor–precipitation relation. *J. Atmos. Sci.*, **74**, 915–931, https://doi.org/10.1175/JAS-D-16-0182.1.

Neelin, J. D., and I. M. Held, 1987: Modeling tropical convergence based on the moist static energy budget. *Mon. Wea. Rev.*, **115**, 3–12, https://doi.org/10.1175/1520-0493(1987)115<0003:MTCBOT>2.0.CO;2.

——, and J. Yu, 1994: Modes of tropical variability under convective adjustment and the Madden–Julian oscillation. Part I: Analytical theory. *J. Atmos. Sci.*, **51**, 1876–1894, https://doi.org/10.1175/1520-0469(1994)051<1876:MOTVUC>2.0.CO;2.

——, O. Peters, and K. Hales, 2009: The transition to strong convection. *J. Atmos. Sci.*, **66**, 2367–2384, https://doi.org/10.1175/2009JAS2962.1.

Peters, O., and J. D. Neelin, 2006: Critical phenomena in atmospheric precipitation. *Nat. Phys.*, **2**, 393–396, https://doi.org/10.1038/nphys314.

Raymond, D. J., 1995: Regulation of moist convection over the west Pacific warm pool. *J. Atmos. Sci.*, **52**, 3945–3959, https://doi.org/10.1175/1520-0469(1995)052<3945:ROMCOT>2.0.CO;2.

——, and X. Zeng, 2000: Instability and large-scale circulations in a two-column model of the tropical troposphere. *Quart. J. Roy. Meteor. Soc.*, **126**, 3117–3135, https://doi.org/10.1002/qj.49712657007.

——, Z. Fuchs, S. Gjorgjievska, and S. L. Sessions, 2015: Balanced dynamics and convection in the tropical troposphere. *J. Adv. Model. Earth Syst.*, **7**, 1093–1116, https://doi.org/10.1002/2015MS000467.

Sobel, A. H., and C. S. Bretherton, 2000: Modeling tropical precipitation in a single column. *J. Climate*, **13**, 4378–4392, https://doi.org/10.1175/1520-0442(2000)013<4378:MTPIAS>2.0.CO;2.

——, S. Wang, and D. Kim, 2014: Moist static energy budget of the MJO during DYNAMO. *J. Atmos. Sci.*, **71**, 4276–4291, https://doi.org/10.1175/JAS-D-14-0052.1.

Wing, A. A., and K. A. Emanuel, 2014: Physical mechanisms controlling self-aggregation of convection in idealized numerical modeling simulations. *J. Adv. Model. Earth Syst.*, **6**, 59–74, https://doi.org/10.1002/2013MS000269.

——, ——, C. E. Holloway, and C. Muller, 2017: Convective self-aggregation in numerical simulations: A review. *Surv. Geophys.*, **38**, 1173–1197, https://doi.org/10.1007/s10712-017-9408-4.

Yano, J.-I., and K. A. Emanuel, 1991: An improved WISHE model of the equatorial atmosphere and its coupling with the stratosphere. *J. Atmos. Sci.*, **48**, 377–389, https://doi.org/10.1175/1520-0469(1991)048<0377:AIMOTE>2.0.CO;2.